The Solution of the Anomalous Diffusion Equation by a
Finite Element Method Formulation
Based on the Caputo Derivative

by

R. M. Corrêa, J. A. M. Carrer *, B. S. Solheid, J. Trevelyan[†]

PPGMNE: Programa de Pós-Graduação em Métodos Numéricos em Engenharia,

Universidade Federal do Paraná, Caixa Postal 19011,

CEP 81531-990, Curitiba, PR, Brasil

[†]Department of Engineering, University of Durham, South Road,

Durham DH1 3LE, UK

corresponding author: carrer@ufpr.br

Abstract

A Finite Element Method formulation is developed for the solution of the anomalous diffusion equation. This equation belongs to the branch of mathematics called fractional calculus; it is governed by a partial differential equation in which a fractional time derivative, whose order ranges in the interval (0,1), replaces the first order time derivative of the classical diffusion equation. In this work, the Caputo integro-differential operator is employed to represent the fractional time derivative. After assuming a linear time variation for the variable of interest, say u, in the intervals in which the overall time is discretized, the integral in the Caputo operator is computed analytically. To demonstrate the usefulness of the proposed formulation, some examples are analysed, showing a good agreement between the FEM results the analytical solutions, even for small orders of the time derivative.

1. Introduction

Although the origins of the *fractional calculus* go back to the origins of the so-called *standard calculus*, only recently a great deal of attention had been given to this branch of mathematics: consequently, a great development was observed both in its theoretical aspects as in what concerns the numerical solutions for problems formulated from the fractional point of view. Initially, the authors would like to mention and recommend the texts entitled Fractional Calculus I, II, III, by Beardon [1], available at the internet, and the report by Loverro [2], as examples of clear and didactic introductions to this thought-provoking matter. Besides, among many others, the textbooks by Miller and Ross [3], Oldham and Spanier [4], Ortigueira [5], Mainardi [6], Klages et al. [7], must be cited. The enlargement of the range of applications is another consequence of the development experienced by the fractional calculus, and an account can be found at Sun et al. [8], Machado et al. [9].

With the aim of enriching the discussion about the use of numerical tools for the solution of problems governed by partial differential equations with fractional time derivative, this work presents a Finite Element Method (FEM) formulation for the solution of the anomalous diffusion problem, with anisotropic media, in two-dimensions. The anomalous, or fractional, diffusion equation presents a time-derivative of non-integer order, that belongs to the interval (0,1). By employing the Greek letter α to represent this non-integer order, then one has, $0 < \alpha < 1$. By using this notation, when $\alpha = 1$ the classical diffusion equation is recovered, which means that it can be treated as the simplest case of the fractional diffusion equation.

Based on the authors' previous works, concerned with the development of Boundary Element Method (BEM) formulations for the solution of the anomalous diffusion equation with the use of the Riemann-Liouville [10] and of the Caputo [11] representations for the fractional time-derivative, the choice in the proposed FEM formulation fell on the latter: in [10], the interested reader can verify that the Riemann-Liouville-based BEM formulation fails in providing accurate results for $\alpha < 0.5$, besides presenting a strong dependence on the time-step length; on the other hand, in [11], the Caputo-based BEM formulation overcame all the deficiencies presented in [10], that is, the formulation in [11] presented accurate results even for α as small as 0.05 and, very important from the computation point of view, an independence from the time-step length. In what concerns the definition of the fractional derivative, the authors would like to call attention to a rather interesting discussion regarding the use of different representations for the fractional space and time derivatives, found in the work by Huang et al. [12]. There the authors state that the definition of the fractional derivative as the Riemann-Liouville operator "has several shortcomings. First, it may cause hyper-singular improper integral. Second, the derivative of a constant is not zero. Third, the fractional derivative involved in the initial condition is often ill-defined." In what

concerns the use of the Caputo operator, one reads: "Besides, the Caputo method does not use the fractional-order derivative in the initial condition, thus is convenient in physical and engineering applications where the initial conditions are usually expressed in terms of the integer-order derivatives." This discussion can be used to justify, in great extent, the differences observed in the BEM results found in references [10] and [11].

The proposed formulation, from now on, will be called CAD-FEM: *C* means Caputo, and *AD*, anomalous diffusion. It is a Galerkin-type formulation. The use of the Caputo representation for the fractional time derivative enables one to obtain the final CAD-FEM equation straightforwardly. It is important to note that the fractional differential operators are non-local, which means that not only the current, but all the previous states, contribute to the determination of a future state of a given system. Consequently, the history contribution must be taken into account, thus generating additional terms, that are summed up, in the CAD-FEM equation. As expected, CAD-FEM is more time-consuming than standard FEM formulations. This drawback cannot be avoided but can be minimized if the proposed formulation is able to present a small dependency on the time-step length: this is what happens with the CAD-FEM, that is to say, the CAD-FEM proved to be efficient from the computational point of view. Additionally, it also proved to be a reliable tool: four examples were included and, in all of them, the CAD-FEM results showed good agreement with the analytical solutions. Details concerning the type of element, the mesh, and the time-step employed in the numerical analyses are given in the corresponding section.

Before finishing this introduction, a brief account of the works concerned with the matter discussed here is given now. Works based on the Finite Difference Method (FDM) appear in a great number, e.g., Murillo and Yuste [13], Meerschaert and Tadjeran [14], Li and Li [15], Çelik and Duman [16]. Other researchers, e.g., Agrawal [17], Deng [18], Huang et al. [12], and Zheng et al. [19], used a framework of the FEM. Using the BEM as the underlying numerical framework, Katsikadelis [20] and Dehghan and Safarpoor [21] must be cited. Meshless formulations have also been employed, see for instance Kumar et al. [22], Zafarghandi et al. [23]. The works referenced here constitute a small parcel of the vast and constantly increasing literature regarding the solution of partial differential equations with fractional derivatives. For this reason, they must be looked upon only as the works that, in some way, influenced the present work. It is not the authors' intention to provide a detailed and comprehensive account of the published works, even because such an enterprise would be impossible.

2. The Anomalous Diffusion Equation

The anomalous diffusion equation, for anisotropic media, reads:

$$\frac{\partial_C^\alpha u}{\partial t^\alpha} = D_x \frac{\partial^2 u}{\partial x^2} + D_y \frac{\partial^2 u}{\partial y^2} \tag{1}$$

In Equation (1), the scalar field, $u = u(x,y,t)$, is function of the space-time variables x,y,t. To shorten the notation, the coordinates (x,y) will be represented by X. Thus, $u = u(X,t)$. Also, D_x and D_y are the constant diffusion coefficients in the x and y directions, respectively.

The fractional derivative $\frac{\partial_C^\alpha u}{\partial t^\alpha}$, $0 < \alpha < 1$, on the left-hand side of Equation (1), according to the Caputo definition is written as:

$$\frac{\partial_C^\alpha u}{\partial t^\alpha} = \frac{1}{\Gamma(1-\alpha)} \int_0^t \frac{1}{(t-\tau)^\alpha} \frac{\partial u(X,\tau)}{\partial \tau} d\tau \tag{2}$$

In Equation (2), $\Gamma(\ldots)$ is the Gamma function.

For a domain Ω, with the boundary Γ represented as: $\Gamma = \Gamma_u \cup \Gamma_q$, the boundary conditions are schematically defined as follows:

Dirichlet boundary condition: $u(X,t) = \hat{u}(X,t)$, over Γ_u \hfill (3)

and

Neumann boundary condition: $q(X,t) = D_x \frac{\partial u}{\partial x} n_x + D_y \frac{\partial u}{\partial y} n_y = \hat{q}(X,t)$, over Γ_q \hfill (4)

In Equation (4), n_x and n_y are the components of the unit outward normal vector to the boundary.

The initial condition is defined as:

$$u(X,0) = u_0(X) \tag{5}$$

3. The Finite Element Method

The Galerkin-based FEM equation, e.g., Bathe [24], Zienkiewicz and Taylor [25], is used as the starting point for the development of the CAD-MEF formulation. As mentioned previously, the classical diffusion equation can be treated as a particular case of a more general equation, which is precisely the fractional diffusion equation.

The FEM equation that corresponds to Equation (1) is written as:

$$Ku = f - M \frac{\partial_C^\alpha u}{\partial t^\alpha} \tag{6}$$

In Equation (6), K is the stiffness matrix, M is the mass matrix, and f is the load vector. If the interpolation, or shape, functions are represented by $N_1, N_2,\ldots,N_n$, then:

$$K = \int_\Omega B^T DB d\Omega \tag{7}$$

$$M = \int_\Omega N^T N d\Omega \tag{8}$$

$$f = \int_\Gamma N^T q d\Gamma \tag{9}$$

where:

$$B = \begin{bmatrix} \dfrac{\partial N_1}{\partial x} & \dfrac{\partial N_2}{\partial x} & \ldots & \dfrac{\partial N_n}{\partial x} \\ \dfrac{\partial N_1}{\partial y} & \dfrac{\partial N_2}{\partial y} & \ldots & \dfrac{\partial N_n}{\partial y} \end{bmatrix} \tag{10}$$

$$D = \begin{bmatrix} D_x & 0 \\ 0 & D_y \end{bmatrix} \tag{11}$$

$$N = \begin{bmatrix} N_1 & N_2 & \ldots & N_n \end{bmatrix} \tag{12}$$

To solve Equation (6), the variable t in Equation (2) is replaced by a discrete value, say $t_{n+1} = (n+1)\Delta t$, where Δt is the selected time interval, and $0 \le t \le t_{n+1}$, and it is assumed that u varies

linearly between two consecutive time steps. This assumption enables one to compute the integral in Equation (2) analytically.

In a more suitable and simplified notation: $u_k = u(X, t_k) = u_k(X)$, one has:

$$u = \frac{(t_{k+1} - \tau)}{\Delta t} u_k + \frac{(\tau - t_k)}{\Delta t} u_{k+1} \tag{13}$$

and consequently:

$$\frac{\partial u}{\partial \tau} = \frac{u_{k+1} - u_k}{\Delta t} \tag{14}$$

Finally, the resulting expression for the Caputo derivative can be written as:

$$\left. \frac{\partial_C^\alpha u}{\partial t^\alpha} \right|_{t=t_{n+1}} = \frac{1}{\Gamma(1-\alpha)} \left[\int_0^{t_1} \frac{1}{(t_{n+1}-\tau)^\alpha} \frac{(u_1 - u_0)}{\Delta t} d\tau + \int_{t_1}^{t_2} \frac{1}{(t_{n+1}-\tau)^\alpha} \frac{(u_2 - u_1)}{\Delta t} d\tau + \ldots + \right.$$
$$\left. \int_{t_k}^{t_{k+1}} \frac{1}{(t_{n+1}-\tau)^\alpha} \frac{(u_{k+1} - u_k)}{\Delta t} d\tau + \ldots + \int_{t_n}^{t_{n+1}} \frac{1}{(t_{n+1}-\tau)^\alpha} \frac{(u_{n+1} - u_k)}{\Delta t} d\tau \right] \tag{15}$$

The integrals in Equation (15) can be computed analytically, and the resulting expression is:

$$\left. \frac{\partial_C^\alpha u}{\partial t^\alpha} \right|_{t=t_{n+1}} = \frac{1}{\Gamma(2-\alpha)\Delta t^\alpha} \left[u_{n+1} - u_n + \sum_{j=0}^{n-1} \left(\frac{1}{(n+1-j)^{\alpha-1}} - \frac{1}{(n-j)^{\alpha-1}} \right) (u_{j+1} - u_j) \right] \tag{16}$$

Equation (16) can be rewritten concisely as:

$$\left. \frac{\partial_C^\alpha u}{\partial t^\alpha} \right|_{t=t_{n+1}} = \frac{1}{\Gamma(2-\alpha)\Delta t^\alpha} \left[u_{n+1} - u_n + \sum_{j=0}^{n-1} B_{(n+1),(j+1)} (u_{j+1} - u_j) \right] \tag{17}$$

where:

$$B_{(n+1),(j+1)} = \frac{1}{(n+1-j)^{\alpha-1}} - \frac{1}{(n-j)^{\alpha-1}} \tag{18}$$

Note that Equation (16) is valid for $n \geq 1$. When $n = 0$, it is written simply as:

$$\left. \frac{\partial_C^\alpha u}{\partial t^\alpha} \right|_{t=t_1} = \frac{1}{\Gamma(2-\alpha)\Delta t^\alpha} \left[u_1 - u_0 \right] \tag{19}$$

Equation (17) can be substituted into Equation (6), written assuming $\boldsymbol{u} = \boldsymbol{u}_{n+1}$:

$$\boldsymbol{K}\boldsymbol{u}_{n+1} = \boldsymbol{f} - \frac{1}{\Gamma(2-\alpha)\Delta t^\alpha} \boldsymbol{M} \left[\boldsymbol{u}_{n+1} - \boldsymbol{u}_n + \sum_{j=0}^{n-1} B_{(n+1),(j+1)} (\boldsymbol{u}_{j+1} - \boldsymbol{u}_j) \right] \tag{20}$$

After applying the boundary conditions to Equation (20), unknown values of u at time t_{n+1}, i.e., u_{n+1}, are determined. Regarding Equation (20), it is important to mention that: *i*) the presence of the summation symbol is due to the non-local behaviour of the Caputo fractional operator: as previously stated, the computation of the current values of u must take into account the history contribution, and *ii*) the factor $B_{(n+1),(j+1)}$ is null when $\alpha = 1.0$, as expected, as this case corresponds to the classical diffusion equation and, consequently, no history contribution must be taken into account.

4. Examples

This section is concerned with the validation of the CAD-FEM formulation. In the four examples, the CAD-FEM results are compared with the analytical solutions. The number of elements employed in the discretization will be denoted by n_Ω, and the number of nodes, by n_{nodes}. For each example, the analyses were carried out with $\alpha = 1.0$, which corresponds to the classical diffusion problem, and with $\alpha = 0.8$, $\alpha = 0.5$, $\alpha = 0.2$, and $\alpha = 0.05$. Reliable results were furnished by the CAD-FEM formulation, even for the two smaller values of α. As expected, some independence on the length of the time-step was observed, with the same Δt being adopted, regardless of the value of α.

4.1. Rectangular Domain with sinusoidal initial condition

In this first example, a bar with length $L = \pi$ is subjected to an initial condition given by:

$$u_0(x) = \sin x \tag{21}$$

The boundary conditions are:

$$u(0,t) = u(\pi,t) = 0 \tag{22}$$

In fact, this is a one-dimensional problem, governed by a simplified version of Equation (1), given below:

$$\frac{\partial_C^\alpha u}{\partial t^\alpha} = D \frac{\partial^2 u}{\partial x^2} \tag{23}$$

By assuming $D = 1.0$, the analytical solution reads, see Murillo and Yuste [13]:

$$u(x,t) = E_\alpha\left(-t^\alpha\right)\sin x \tag{24}$$

In equation (24), $E_\alpha(...)$ is the Mittag-Leffler function, see, for instance, Loverro [2], defined according to:

$$E_\alpha(z) = \sum_{k=0}^{\infty} \frac{z^k}{\Gamma(1+\alpha k)} \tag{25}$$

where $z \in C$, and α is the fractional order of the derivative.

For $\alpha = 1.0$, Equation (25) reduces to:

$$E_1(z) = e^z \tag{26}$$

and Equation (24) becomes the well-known, and quite simple, the analytical solution for the classical diffusion

$$u(x,t) = e^{-t}\sin x \tag{27}$$

For the simulation of this one-dimensional problem through the two-dimensional CAD-FEM, a rectangular domain constituted of an isotropic medium with $D_x = D_y = D = 1$, and defined over the region $0 \leq x \leq \pi$ and $0 \leq y \leq \pi/2$, was adopted. Dirichlet and Neumann boundary conditions are required for a successful simulation, and are written below:

$$u(0, y, t) = u(\pi, y, t) = 0 \tag{28}$$

and

$$q(x, 0, t) = q(x, \pi/2, t) = 0 \tag{29}$$

Equations (28) and (29) make clear the independence of the variable u regarding the y direction.

The initial condition now reads:

$$u_0(x, y) = \sin x \tag{30}$$

The mesh displayed in Figure 1 was adopted to perform the CAD-FEM analyses. It has $n_\Omega = 128$ linear quadrangular elements and $n_{nodes} = 153$. The time-step is $\Delta t = 0.005$. The results for $u(\pi/2, \pi/4, t)$ are depicted in Figure 2, whereas the results along the x-axis, $y = \pi/4$, for the selected times $t_s = 0.25$ and $t_s = 2.0$, are found in Figures 3 and 4. From Figures 2 – 4, one can notice a good agreement between the CAD-FEM results and the analytical solution for each of the chosen values of α, bringing some optimism in what concerns the capability of the CAD-FEM of furnishing accurate results even for more complex analyses.

4.2. Rectangular Domain with Dirichlet boundary conditions

This is another one-dimensional problem, that can be interpreted as a heat transfer from the region at $x = 0$, where $\hat{u} = 10$, to the region at $x = L$, where $\hat{u} = 0$. The initial condition is null. Again, the one-dimensional problem was simulated with the analyses being carried out in a rectangular domain defined over the region $0 \le x \le L$ and $0 \le y \le L/2$, now with $L = 2$. The same mesh of the first example was adopted, only scaled to accommodate the different domain sizes.

For the rectangular domain, the Dirichlet and the Neumann boundary conditions are given, respectively, by Eqs. (31) and (32) below:

$$u(0, L/2, t) = 10, \quad u(L, y, t) = 0 \tag{31}$$

and

$$q(x, 0, t) = q(x, L/2, t) = 0 \tag{32}$$

The initial condition is:

$$u_0(x, y) = 0 \tag{33}$$

The analyses were carried out with $D_x = D_y = D = 1.0$, all with $\Delta t = 0.005$. Results for $u(L/2, L/4, t)$ are presented in Figure 5. Results along the x-axis, $y = 1$, for $t_s = 0.25$ and $t_s = 1.0$ are presented in Figures 6 and 7, respectively. A comparison between the CAD-FEM results and the analytical solution, given by:

$$u(x, t) = U_0 \left(1 - \frac{x}{L} \right) - \frac{2U_0}{\pi} \sum_{k=1}^{\infty} \frac{1}{k} E_\alpha \left(-\left(\frac{k\pi}{L} \right)^2 Dt^\alpha \right) \sin\left(\frac{k\pi x}{L} \right) \tag{34}$$

showed a good agreement between them.

The computation of the analytical values cannot be accomplished straightforwardly, once the argument of the Mittag-Leffler function in Eq. (34) grows faster than the converge of the series and, even for a small k, the number of the terms in Mittag-Leffler series became prohibitively large. However, with the use of the algorithm found at https://github.com/khinsen/mittag-leffler, which is

a Python language version of a MATLAB® routine presented by Garrappa [26], this drawback was successfully overcame.

4.3. Circular Domain with Dirichlet Boundary Condition

This third example can be succinctly characterized as follows: it is constituted by an isotropic circular domain of radius R, with null initial condition and with a constant Dirichlet boundary condition over the entire Γ. From the above description, the problem is better represented mathematically after adopting a polar coordinate system (r,θ): now, $u = u(r,t)$, and Equation (1) is rewritten as:

$$\frac{\partial_C^\alpha u}{\partial t^\alpha} = D \left(\frac{\partial^2 u}{\partial r^2} + \frac{1}{r}\frac{\partial u}{\partial r} \right) \tag{35}$$

Note that Eq. (35) describes an axisymmetric problem with an isotropic medium.

In the polar coordinate system, the domain is defined according to $0 \le r \le R$ and $0 \le \theta \le 2\pi$, and the null initial condition and the Dirichlet boundary condition are written, respectively, as:

$$u_0(r,\theta) = 0 \tag{36}$$

and

$$u(R,\theta,t) = \hat{u} \tag{37}$$

The analytical solution reads:

$$u(r,t) = \hat{u} - \frac{2\hat{u}}{R} \sum_{n=1}^{\infty} \frac{J_0(\lambda_n r)}{\lambda_n J_1(\lambda_n R)} E_\alpha \left(-D\lambda_n^2 t^\alpha \right) \tag{38}$$

where $J_0(...)$ and $J_1(...)$ are Bessel functions of the first kind and orders zero and one, respectively, and the parameters λ_n are the positive roots of the equation

$$J_0(\lambda_n R) = 0 \tag{39}$$

The analyses were carried out with $D = 1.0$, $R = 10$, and $\hat{u} = 10$. The mesh, depicted in Figure 8, was generated by GMSH©, see Geuzaine C and Remacle [27]; it has $n_\Omega = 2806$ six-nodes triangular elements and $n_{nodes} = 5741$. The selected time-step is $\Delta t = 0.1$.

Results for $u(r,t_s)$, with $t_s = 1.0, 4.0, 20.0, 60.0$, are depicted in Figures 9 – 13 for $\alpha = 1.0$, 0.8, 0.5, 0.2, 0.05, respectively. Results for $u(5,t)$ are depicted in Figure 14. Figures 9 – 14 provide a good description of the influence of α in the results: as the values of α decrease, the same happen with the values of u, for $r < R$. Also, it can be observed that the curves for different times become closer to each other with increasing gradients towards the boundary. The results for $\alpha = 0.05$ fit quite well in this description. At the end of the first example, the authors made a brief comment about their optimism with the capability of the CAD-FEM to provide accurate results, even to more complex problems. That optimism proved to be not exaggerated, as attested by the results presented here, which are in good agreement with the not trivial analytical solution in Equation (38).

4.4. Square domain with initial sinusoidal condition

This last example consists of a square domain defined over the region $0 \le x,y \le L$. The boundary conditions are:

$$u(0, y,t) = u(L, y,t) = u(x,0,t) = u(x,L,t) = 0 \tag{40}$$

The initial condition is defined according to:

$$u_0(x, y) = \sin\left(\frac{\pi x}{L}\right)\sin\left(\frac{\pi y}{L}\right) \tag{41}$$

The analytical solution, for an anisotropic medium, reads:

$$u(x, y,t) = E_\alpha\left(-v^2 t^\alpha\right)\sin\left(\frac{\pi x}{L}\right)\sin\left(\frac{\pi y}{L}\right) \tag{42}$$

with:

$$v = \frac{\pi}{L}\sqrt{D_x + D_y} \tag{43}$$

Two media were considered: one isotropic, with $D_x = D_y = 1.0$, and one anisotropic, with $D_x = 1.0$ and $D_y = 0.1$. For both media, $L = 10$.

In this last example, with the aim of providing a more comprehensive discussion regarding the FEM results accuracy, a convergence study is also included. This study consists in computing the relative L^2 error norm, E_2, for different meshes with increasing number of elements. The following formula was adopted:

$$E_2 = \frac{\left\|u_{analytical} - u_{FEM}\right\|_{L^2(\Omega)}}{\left\|u_{analytical}\right\|_{L^2(\Omega)}} = \frac{\sqrt{\int_\Omega \left(u_{analytical} - u_{FEM}\right)^2 d\Omega}}{\sqrt{\int_\Omega \left(u_{analytical}\right)^2 d\Omega}} \cong \frac{\sqrt{\sum_{i=1}^{N}\left(u_{analytical}^i - u_{FEM}^i\right)^2}}{\sqrt{\sum_{i=1}^{N}\left(u_{analytical}^i\right)^2}} \tag{44}$$

where the analytical and the FEM solutions are represented, respectively, by $u_{analytical}$ and u_{FEM}.

Three FEM meshes were employed. The first mesh has $n_\Omega = 100$ linear quadrangular elements and $n_{nodes} = 121$, see Figure 15; for the second mesh, one has $n_\Omega = 400$ and $n_{nodes} = 441$, see Figure 15 and, finally, the third and more refined mesh, depicted in Figure 17, has $n_\Omega = 1600$ and elements and $n_{nodes} = 1681$. For $t_s = 10$ and $t_s = 15$, the convergence study results are depicted in Figures 18 – 19, for the isotropic medium, and in Figures 20 – 21, for the anisotropic medium. BEM results, included for enriching the discussion in Figures 18 – 21, were also obtained employing three different meshes, in such a way that to each one of the FEM meshes does correspond a BEM mesh that has the same number of nodes. It should be noted, however, that the number of linear triangular cells in the BEM meshes are always twice the number of linear quadrangular finite elements, see Carrer et al. [11]. A careful examination of Figures 18 – 21 enables one to conclude that although the use of more refined meshes produced very similar results for the error E_2 for both FEM and BEM, in general the FEM errors are smaller than the BEM corresponding ones for the less refined meshes. Two notable exceptions to this conclusion should be mentioned. Amazingly, these exceptions occurred for $\alpha = 1$, that is, for the classical diffusion problem, and are readily seen in Figure 19, where the FEM error is greater than the corresponding BEM error, and in Figure 20, where the BEM error stood much greater than all the others, not converging for an apparently common value. Regarding Figures 18 – 21, note that BEM results present a higher rate of convergence than FEM results. Relatively to the CPU time, the comparison between FEM and BEM cannot be made, as the FEM analyses were carried out using a computer code developed in the Python language, whereas for the BEM analyses the computer code used the FORTRAN language.

In all the analyses, the same time-step, $\Delta t = 0.05$, was employed, regardless the mesh.

The results for $u(L/2, L/2, t)$ and $u(x, 5, 10)$, are depicted in Figures 22 and 24, for the isotropic medium, and in Figures 23 and 25, for the anisotropic medium. Finally, Figures 26 and 27 present the results of $u(x, y, 10)$ for the two media. Once again, the CAD-FEM results are in good agreement with the analytical solution.

Conclusions

A FEM formulation, called CAD-FEM, has been presented for the numerical solution of the anomalous diffusion problem, with anisotropic media, in two dimensions. This problem is governed by a partial differential equation with a fractional time derivative of order α, with $0 < \alpha < 1$. If, in the governing equation, one assumes $\alpha = 1$, then the classical diffusion equation is recovered. One of the pursued objectives of this work was the development of a formulation capable of providing reliable results, even for small orders of the fractional time derivative, that is, for small values of α. Another task that deserved attention was related to the computational efficiency, due to the non-local behaviour of the fractional operators. The use of the Caputo operator turned possible the development of such a formulation: the CAD-FEM meets the two above pursued objectives, as reliable results were obtained for fractional derivatives as small as 0.05, and the time-marching process demonstrated independence on the time-step length, with all the analyses, in each example, being carried out with the same Δt. The results presented here are encouraging and, no doubt, stimulate the continuity of this research. Further improvements directed towards the reduction in the computer time are always desirable and remain the subject of future research: one possibility that seems plausible to achieve this goal is the use of increasing variable time-steps, mainly when the solution of the problem is reaching the steady-state. The diffusion-advection problem, whose governing equation presents space fractional derivatives, is a matter that also deserves attention and, indeed, is a challenge to be faced soon. Anyway, it was demonstrated here that the FEM can be used as a powerful tool in the solution of fractional calculus problems.

References

[1] Beardon A. Fractional Calculus I, available at https://nrich.maths.org/1365/index, Fractional Calculus II, available at https://nrich.maths.org/1369, Fractional Calculus III, available at https://nrich.maths.org/1371, 2000.

[2] Loverro A. *Fractional Calculus: History, Definitions and Applications for the Engineer*. Department of Aerospace and Mechanical Engineering University of Notre Dame, 2004

[3] Miller KS, Ross B. *An Introduction to the Fractional Calculus and Fractional Differential Equations*, Wiley-Interscience, 1993.

[4] Oldham KB, Spanier J. *The Fractional Calculus. Theory and Applications of Differentiation and Integration to Arbitrary Order*, Academic Press, Inc., 1974.

[5] Ortigueira MD. *Fractional Calculus for Scientists and Engineers*, Lecture Notes in Electrical Engineering, volume 84, 2011, Springer.

[6] Mainardi F. *Fractional Calculus: Theory and Applications*. Printed edition of the special issue published in *Mathematics*, Mdpi AG, 2018.

[7] Klages R, Radons G, Sokolov IM (eds.). *Anomalous Transport, Foundations and Applications*. WILEY-VCH Verlag GmbH & Co. KGaA, 2008.

[8] Sun H, Zhang Y, Baleanu D, Chen W, Chen Y. A new collection of real world applications of fractional calculus in science and engineering. Communications in Nonlinear Science and Numerical Simulation 2018; **64**, 213–31.

[9] Machado JAT, Silva MF, Barbosa RS, Jesus IS, Reis CM, Marcos MG, Galhano AF. Some Applications of Fractional Calculus in Engineering. *Mathematical Problems in Engineering*, 2010, Article ID 639801, 34 pages, doi:10.1155/2010/639801

[10] Carrer JAM, Seaid M, Trevelyan J, Solheid BSS. The boundary element method applied to the solution of the anomalous diffusion problem, *Engineering Analysis with Boundary Elements*, 2019; **109**, 129-142.

[11] Carrer JAM, Solheid BS, Trevelyan J, Seaid M. A boundary element method formulation based on the Caputo derivative for the solution of the anomalous diffusion problem, *Engineering Analysis with Boundary Elements*, 2021; **122**, 132-144.

[12] Huang Q, Huang G, Zhan H. A Finite Element Solution for the Fractional Advection-Dispersion Equation, *Advances in Water Resources*, 2008; **31**, 1578-1589.

[13] Murillo JQ, Yuste SB. An Explicit Difference Method for Solving Fractional Diffusion and Diffusion-Wave Equations in the Caputo Form, *Journal of Computational and Nonlinear Dynamics*, 2011; **6**, on line.

[14] Meerschaert MM, Tadjeran C. Finite Difference Approximations for Fractional Advection-Dispertion Flow Equations, *Journal of Computational and Applied Mathematics*, 2004; **172**, 65-77.

[15] Li W, Li C. Second Order Explicit Difference Schemes for the Space Fractional Advection Diffusion Equation, *Applied Mathematics and Computation*, 2015; **257**, 446-457.

[16] Çelic C, Duman M. Crank-Nicholson Method for the Fractional Diffusion Equation with the Riesz Fractional Derivative, *Journal of Computational Physics*, 2012; **231**, 1743-1750.

[17] Agrawal OP. A General Finite Element Formulation for Fractional Variational Problems, *Journal of Mathematical Analysis and Applications*, 2008; **337**, 1-12.

[18] Deng WH. Finite Element Method for the Space and Time Fractional Fokker-Planck Equation, *SIAM Journal on Numerical Analysis*, 2008; **47**, 204-226.

[19] Zheng Y, Li C, Zhao Z. A Note on Finite Element Method for the Space-Fractional Advection Diffusion equation, *Computers and Mathematics with Applications*, 2010; **59**, 1718-1726.

[20] Katsikadelis JT. The BEM for Numerical Solution of Partial Fractional Differential Equations, *Computers and Mathematics with Applications*, 2011; **62**, 891-901.

[21] Dehghan M, Safarpoor M. The Dual Reciprocity Boundary Elements Method for the Linear and Nonlinear Two-Dimensional Time-Fractional Partial Differential Equations, *Mathematical Methods in the Applied Sciences*, 2016, **39**, 3979-3995.

[22] Kumar A, Bhardwaj A, Kumar BVR. A meshless local collocation method for time fractional diffusion wave equation. *Computers and Mathematics with Applications*, 2019; **78**, 1851-1861.

[23] Zafarghandi FS, Mohammadi M, Babolian E, Javadi S. Radial Basis Functions Method for Solving the Fractional Diffusion Equations. *Applied Mathematics and Computation*, 2019; **342**, 224-246.

[24] Bathe KJ. *Finite element procedures*. Prentice Hall, New Jersey, 1996.

[25] Zienkiewicz, OC and Taylor, RL. *The finite element method for solid and structural mechanics*. Elseiver Butterworth-Heinemann, 6th edition, 2006.

[26] Garrappa R. Numerical evaluation of two and three parameter Mittag-Leffler functions, *SIAM Journal of Numerical Analysis*, 2015; **53**, 1350-1369.

[27] Geuzaine C and Remacle JF. Gmsh: A 3-D finite element mesh generator with built-in pre- and post-processing facilities. *International Journal for Numerical Methods in Engineering*, 2009, **79**, 1309-1331.

Caption to the Figures

Figure 1. Rectangular mesh with $n_\Omega = 128$ linear quadrangular elements and $n_{nodes} = 153$, employed in the first and in the second examples.

Figure 2. Domain under initial condition: results for $u(\pi/2,\pi/4,t)$.

Figure 3. Domain under initial condition: results for $u(x,\pi/4,0.25)$.

Figure 4. Domain under initial condition: results for $u(x,\pi/4,2.0)$.

Figure 5. Domain with Dirichlet boundary conditions: results at $u(L,L/2,t)$.

Figure 6. Domain with Dirichlet boundary conditions: results at $u(x,L/2,0.25)$.

Figure 7. Domain with Dirichlet boundary conditions: results at $u(x,L/2,1.0)$.

Figure 8. Circular domain: mesh with $n_\Omega = 2806$ six-node triangular elements and $n_{nodes} = 5741$.

Figure 9: Circular domain: results for $u(r,t_s)$, with $t_s = 1.0, 4.0, 20.0, 60.0$, and $\alpha = 1.0$.

Figure 10: Circular domain: results for $u(r,t_s)$, with $t_s = 1.0, 4.0, 20.0, 60.0$, and $\alpha = 0.8$.

Figure 11: Circular domain: results for $u(r,t_s)$, with $t_s = 1.0, 4.0, 20.0, 60.0$, and $\alpha = 0.5$.

Figure 12: Circular domain: results for $u(r,t_s)$, with $t_s = 1.0, 4.0, 20.0, 60.0$ and $\alpha = 0.2$.

Figure 13: Circular domain: results for $u(r,t_s)$, with $t_s = 1.0, 4.0, 20.0, 60.0$, and $\alpha = 0.05$.

Figure 14: Circular domain: results for $u(5,t)$.

Figure 15. Square Domain: mesh $n_\Omega = 100$ linear quadrangular elements and $n_{nodes} = 121$.

Figure 16. Square Domain: mesh $n_\Omega = 400$ linear quadrangular elements and $n_{nodes} = 441$.

Figure 17. Square Domain: mesh $n_\Omega = 1600$ linear quadrangular elements and $n_{nodes} = 1681$.

Figure 18. Square domain, isotropic medium: convergence study at t = 10.

Figure 19. Square domain, isotropic medium: convergence study at t = 15.

Figure 20. Square domain, anisotropic medium: convergence study at t = 10.

Figure 21. Square domain, anisotropic medium: convergence study at t = 15.

Figure 22. Square domain: isotropic medium, results for $u(L/2,L/2,t)$.

Figure 23. Square domain: anisotropic medium, results for $u(L/2,L/2,t)$.

Figure 24. Square domain: isotropic medium, results for $u(x,L/2,10)$.

Figure 25. Square domain: isotropic medium, results for $u(x,L/2,10)$.

Figure 26. Square domain: isotropic medium, results for $u(x,y,10)$. (a) $\alpha = 1.0$, (b) $\alpha = 0.8$, (c) $\alpha = 0.5$, (d) $\alpha = 0.2$, (e) $\alpha = 0.05$.

Figure 27. Square domain: isotropic medium, results for $u(x,y,10)$. (a) $\alpha = 1.0$, (b) $\alpha = 0.8$, (c) $\alpha = 0.5$, (d) $\alpha = 0.2$, (e) $\alpha = 0.05$.
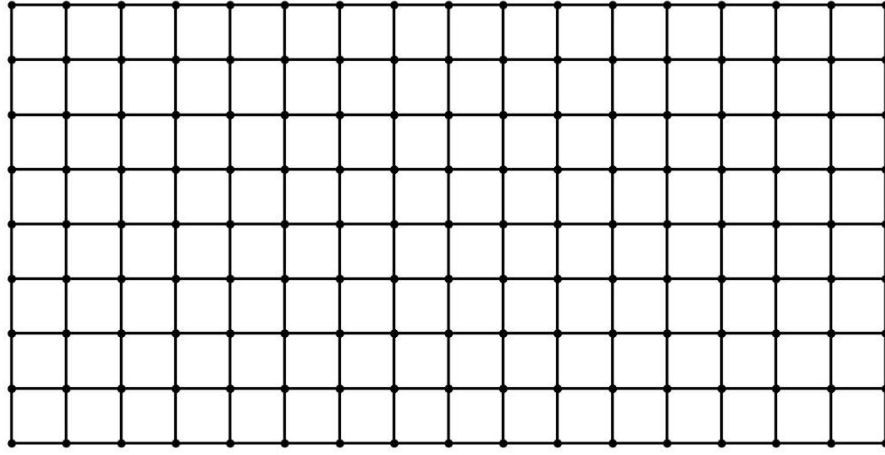
Figure 1
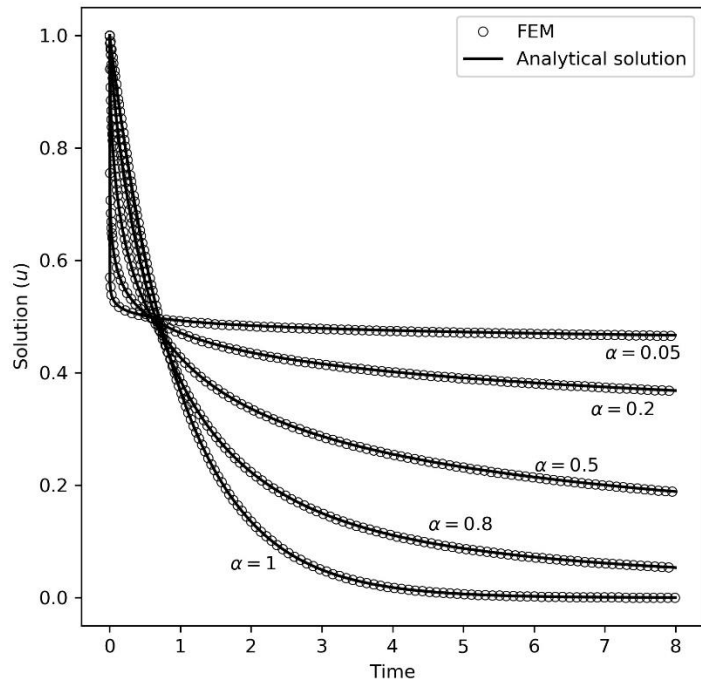
Figure 2
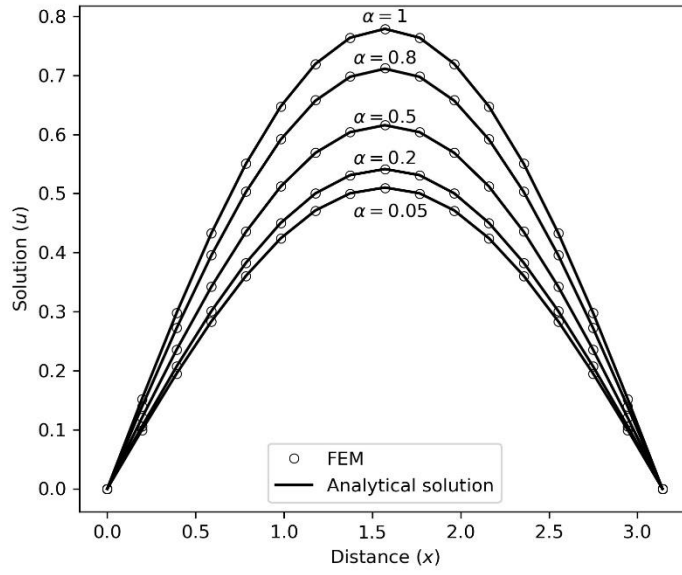
Figure 3
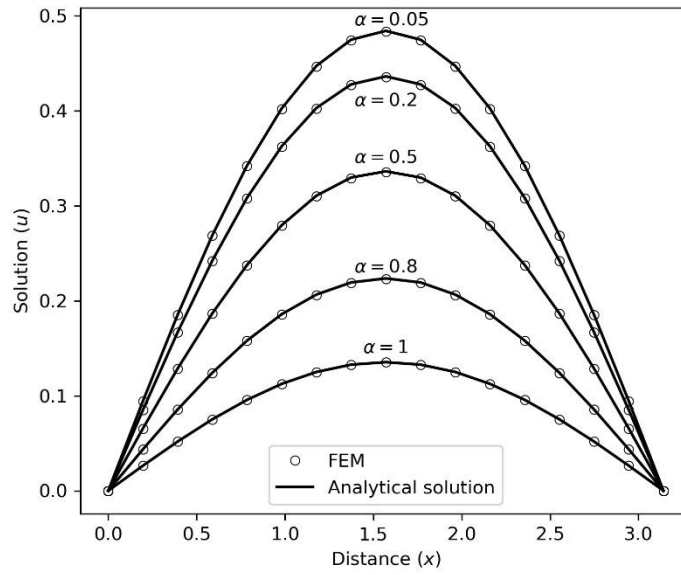
Figure 4
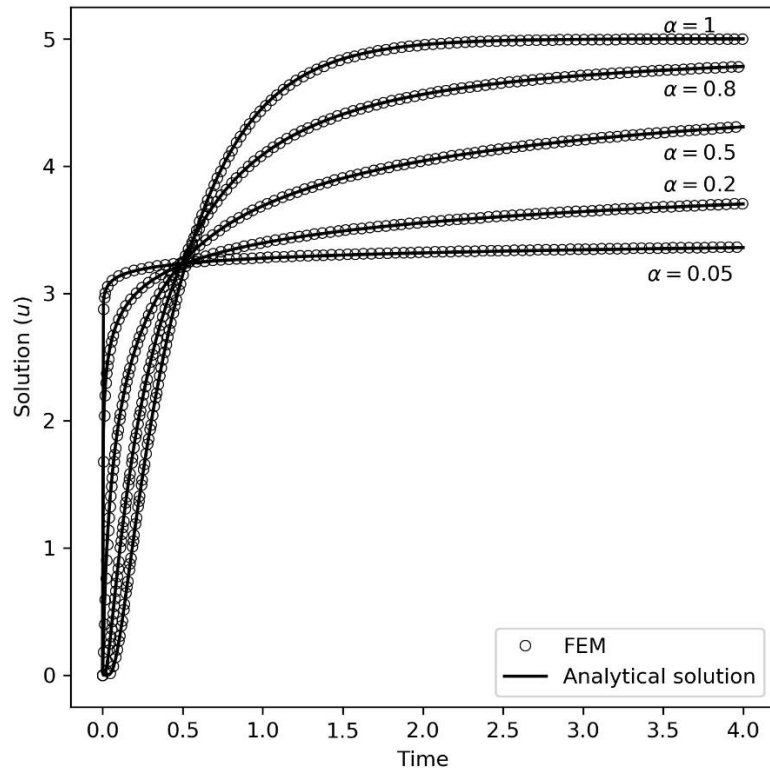
Figure 5
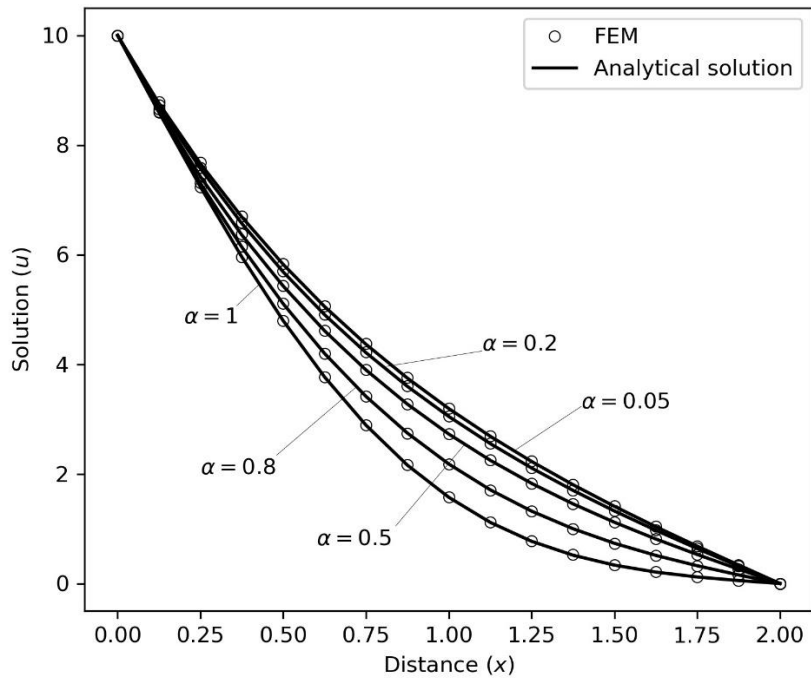
Figure 6
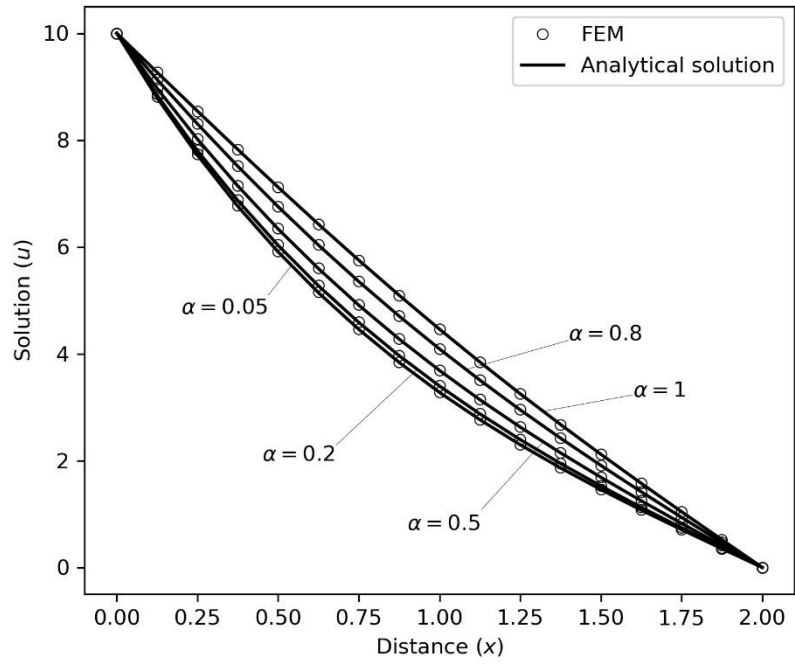
Figure 7
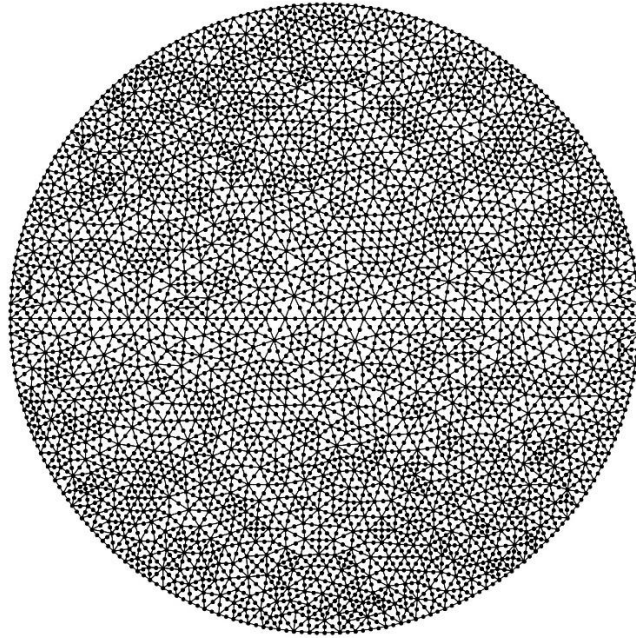
Figure 8
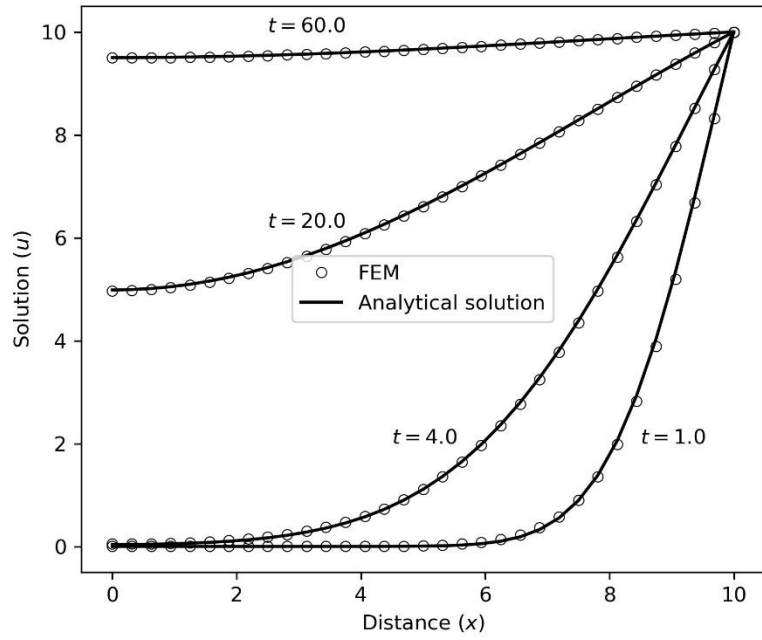
Figure 9
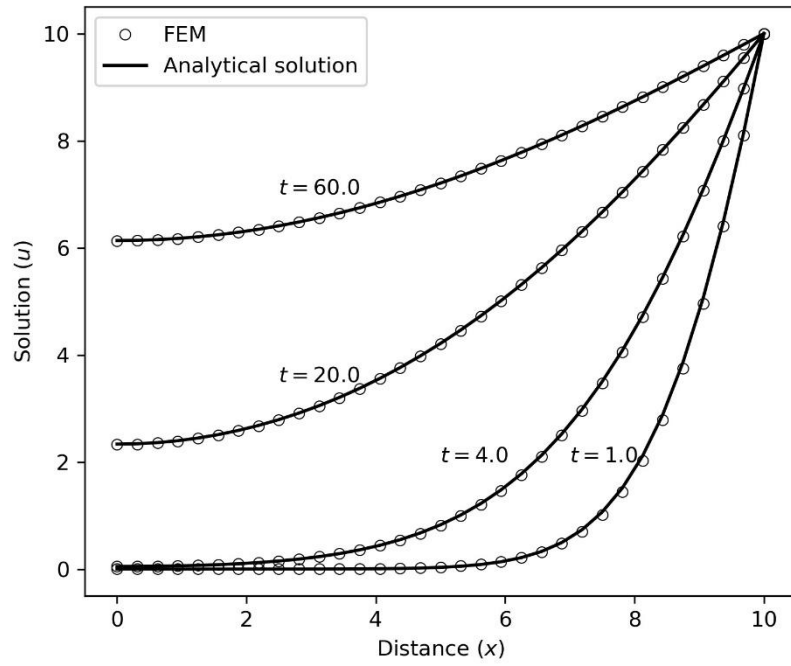
Figure 10
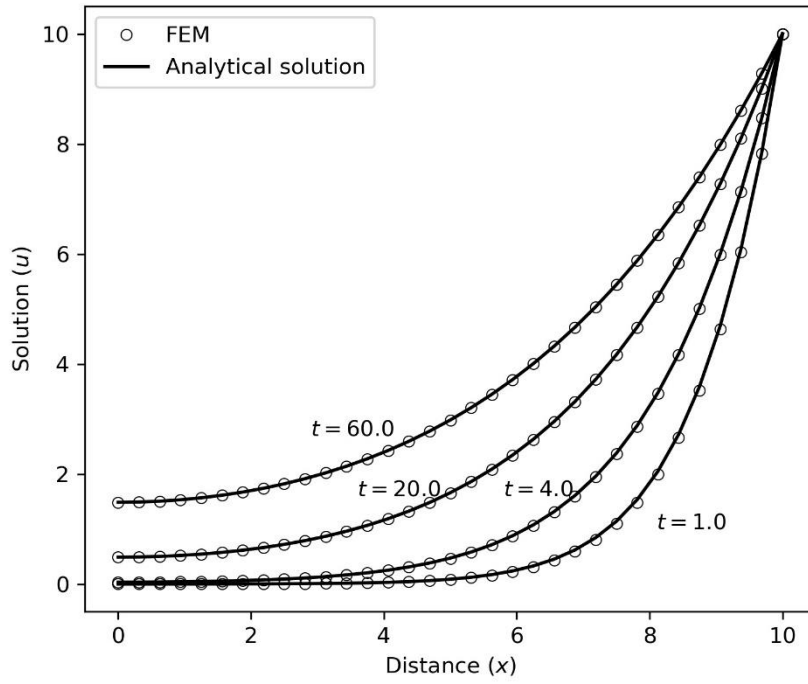
Figure 11
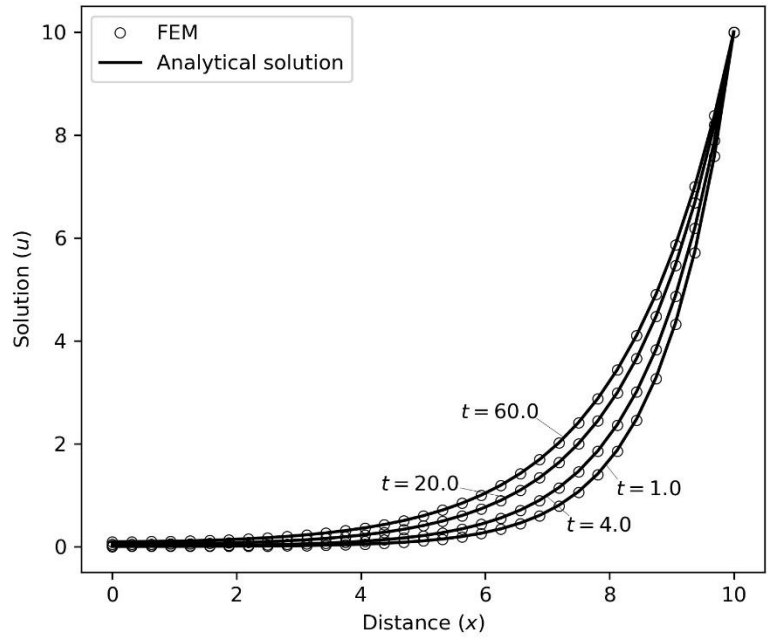
Figure 12
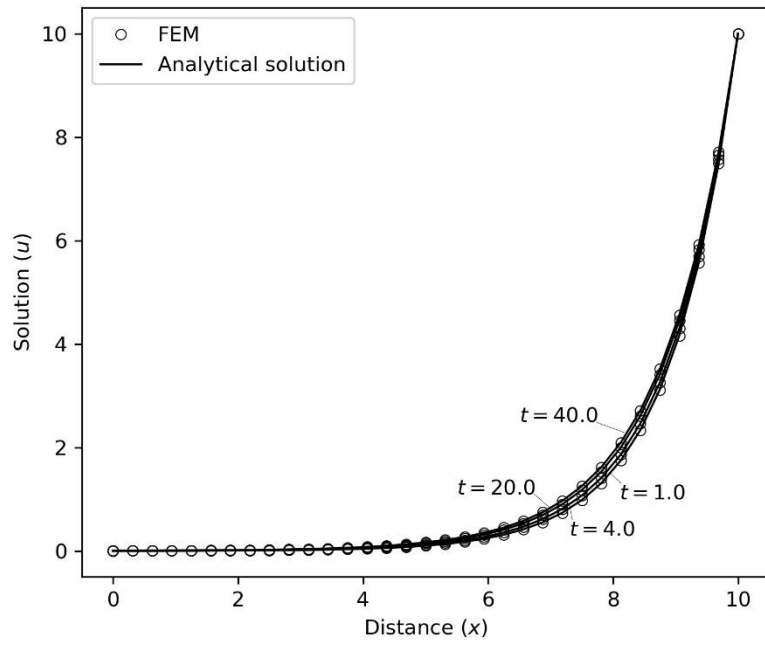
Figure 13
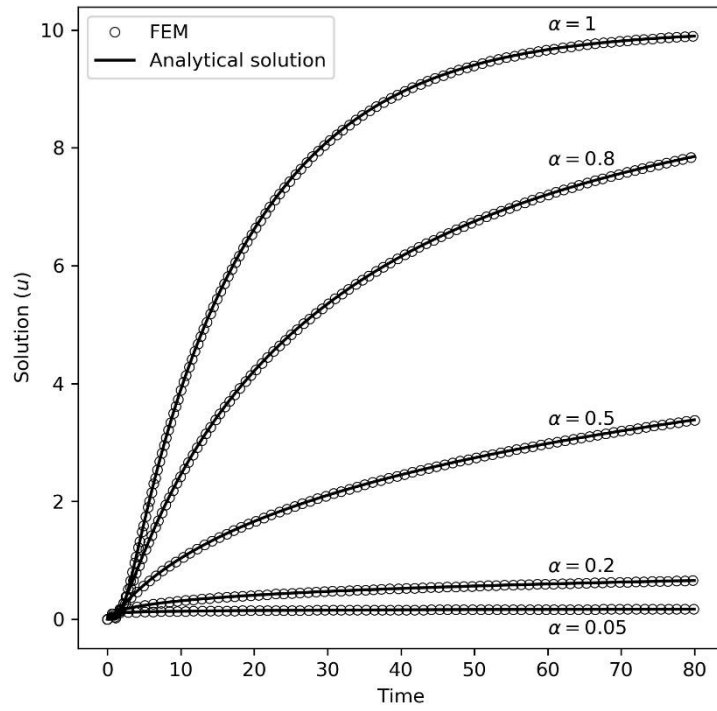
Figure 14
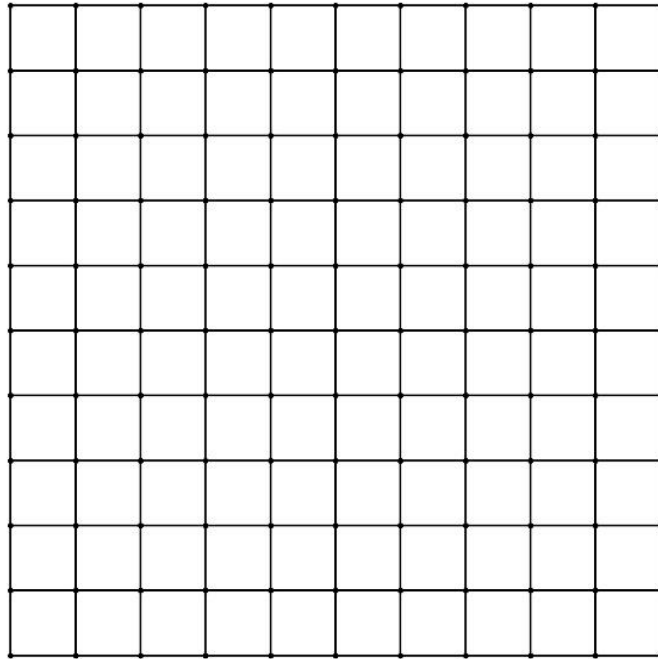
FIGURE 15
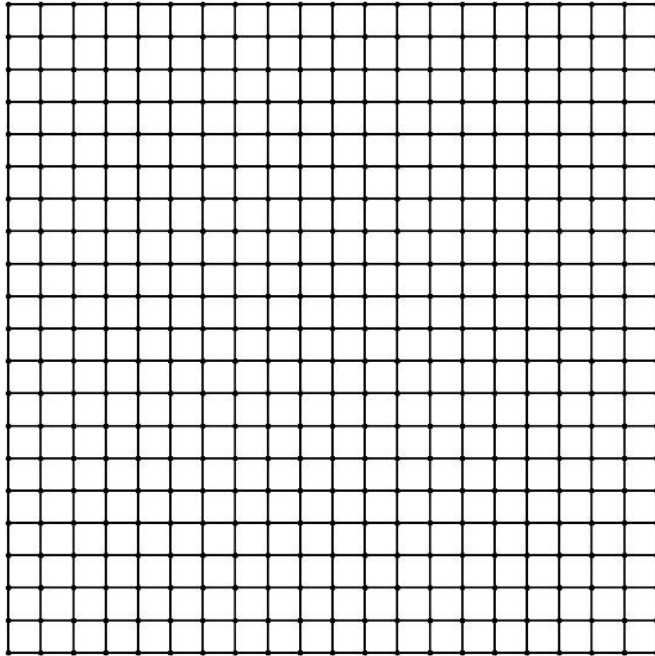
FIGURE 16
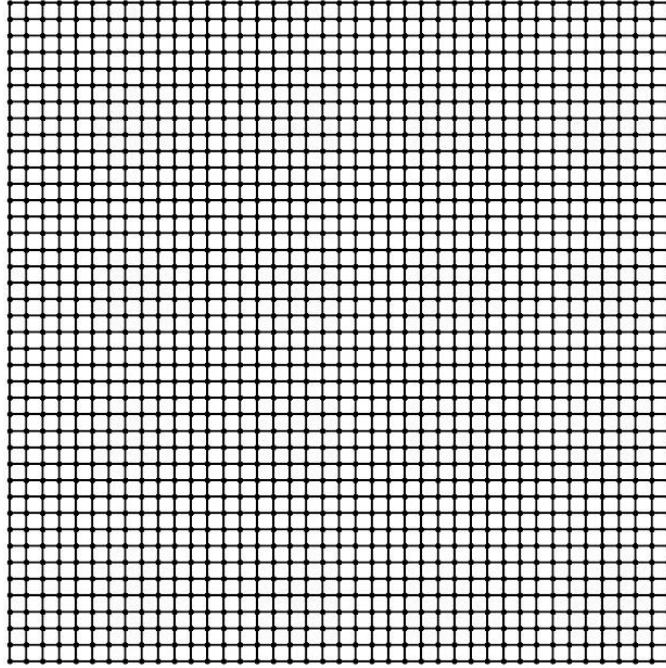
Figure 17
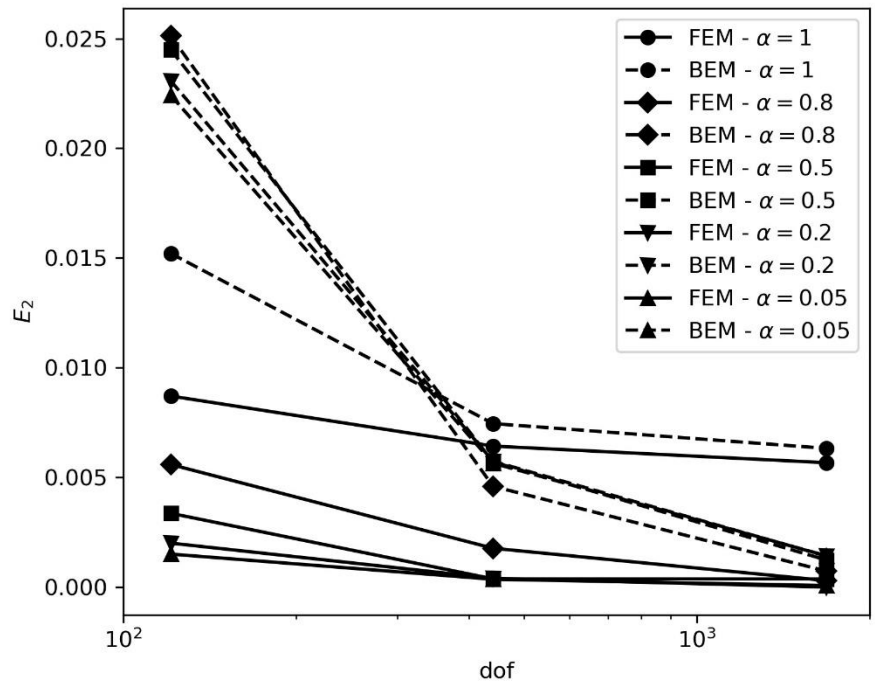
FIGURE 18
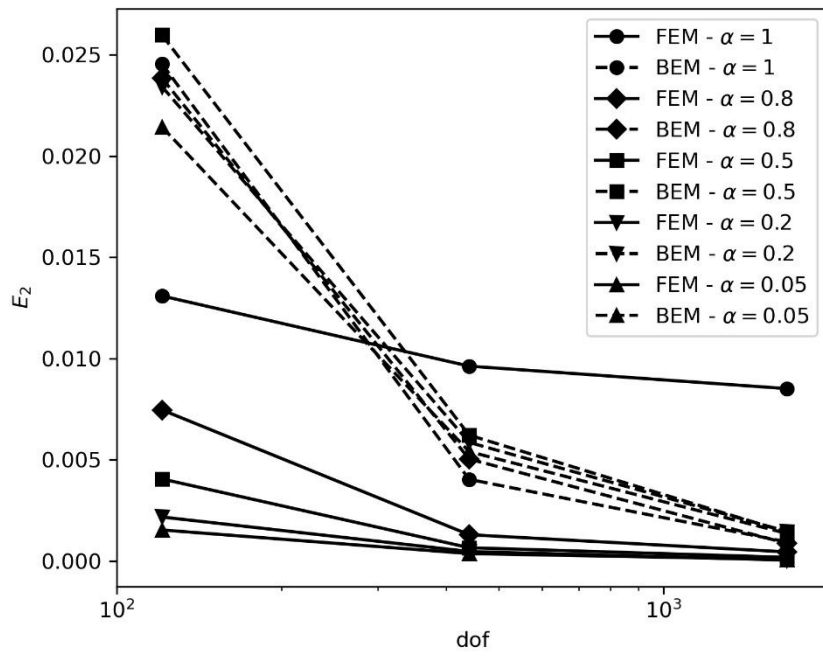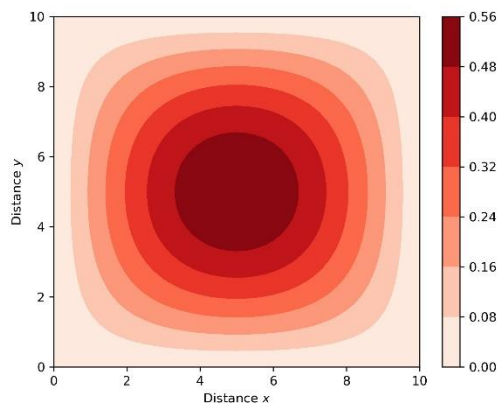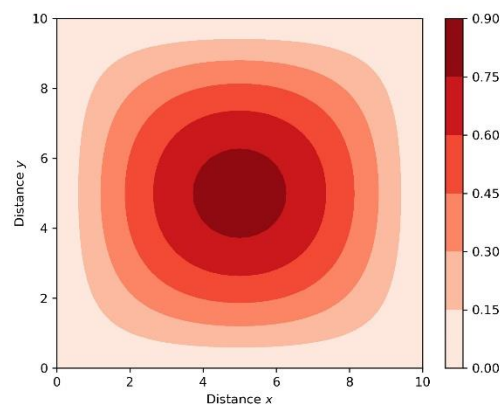
FIGURE 19
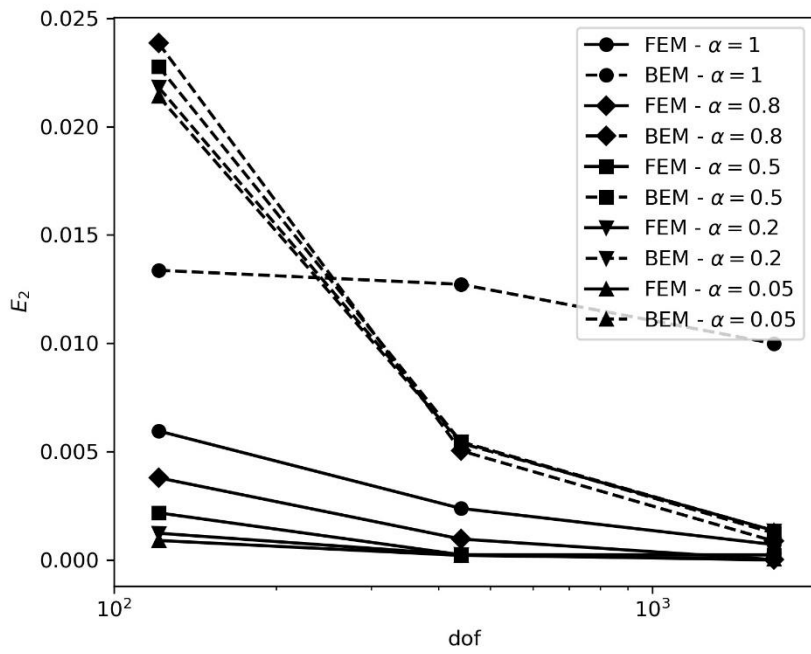
FIGURE 20
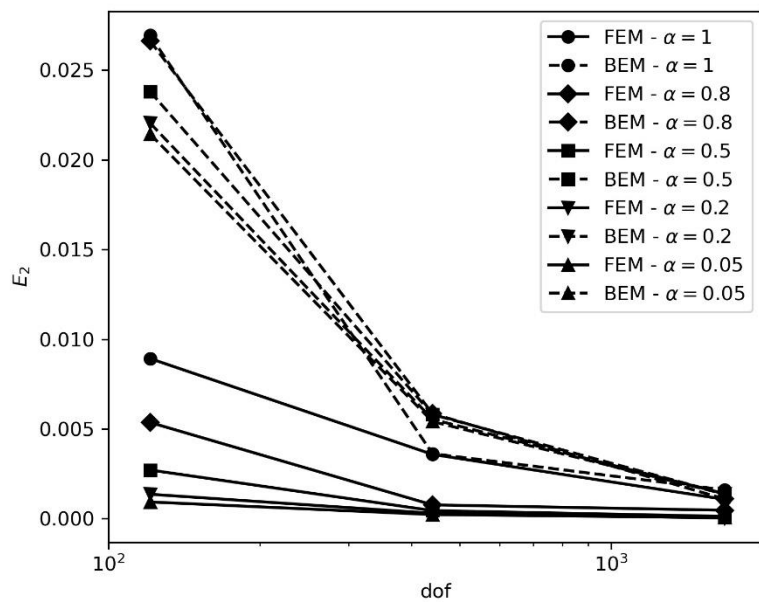
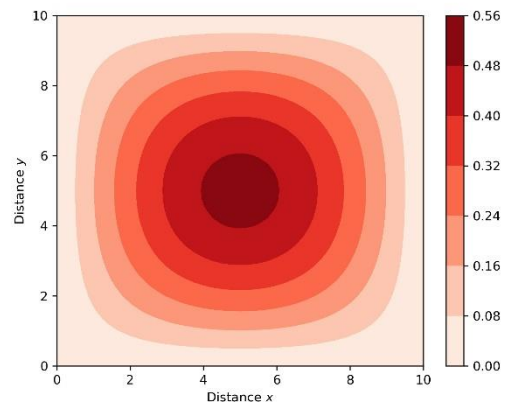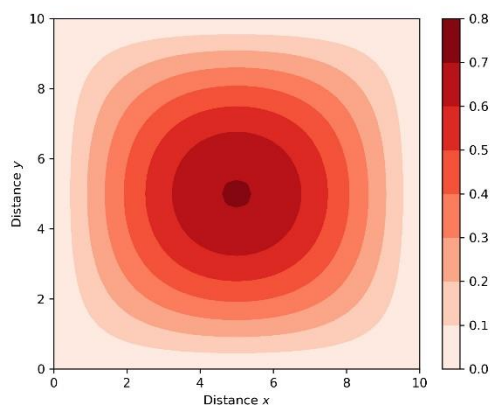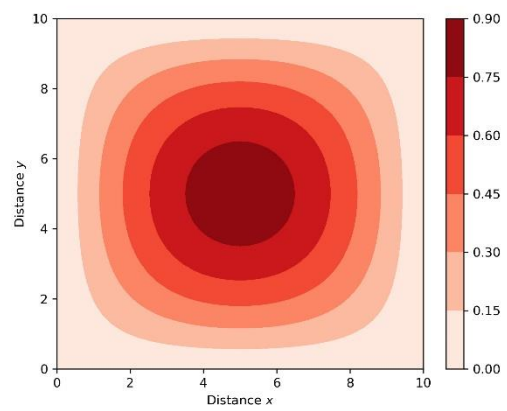FIGURE 21
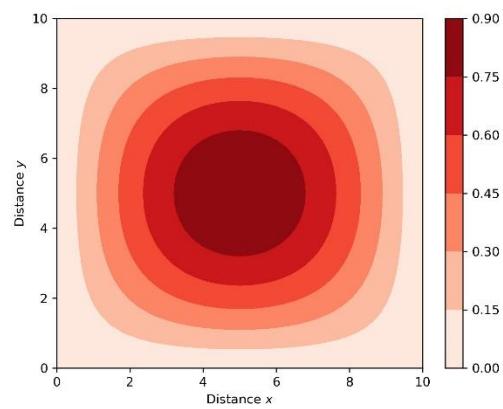
Figure 15
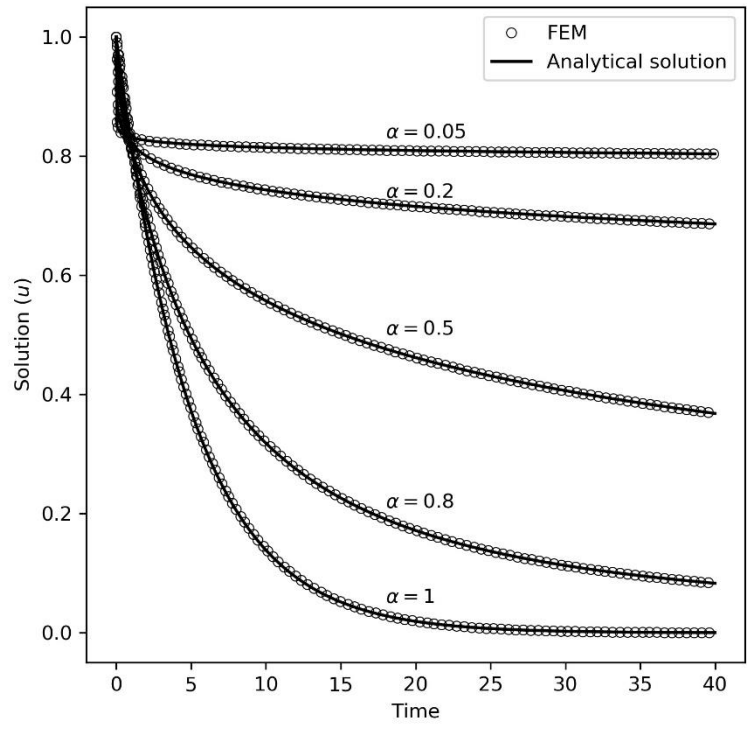
Figure 22
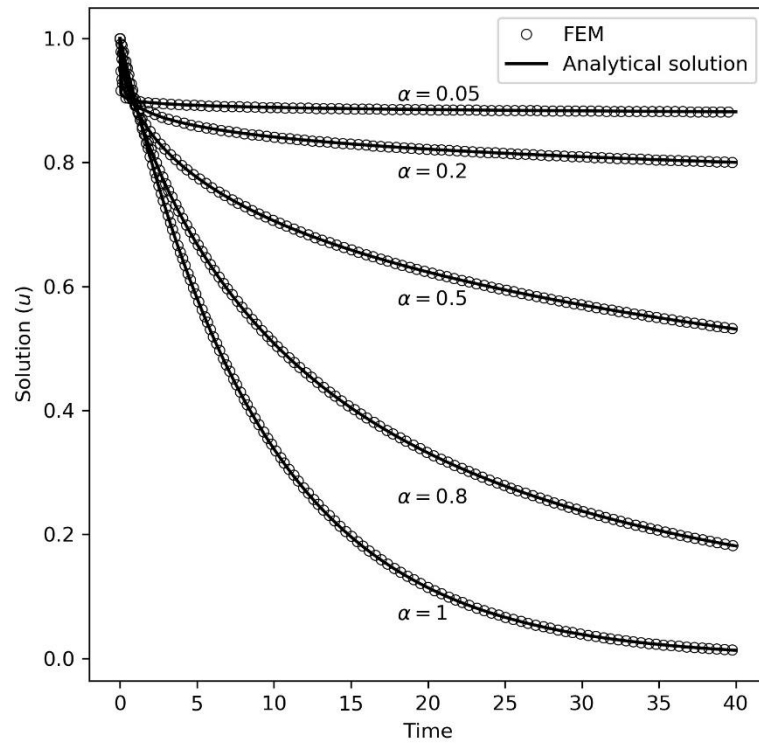
Figure 23
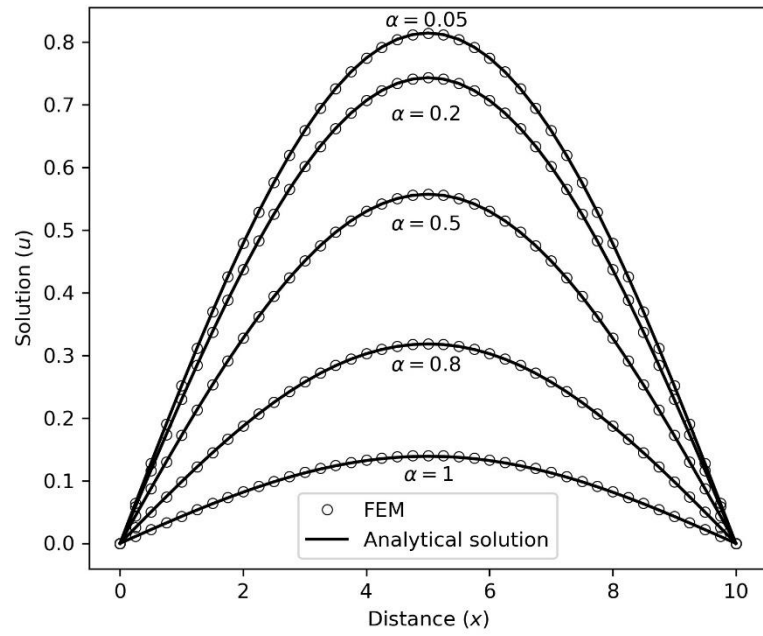
Figure 24
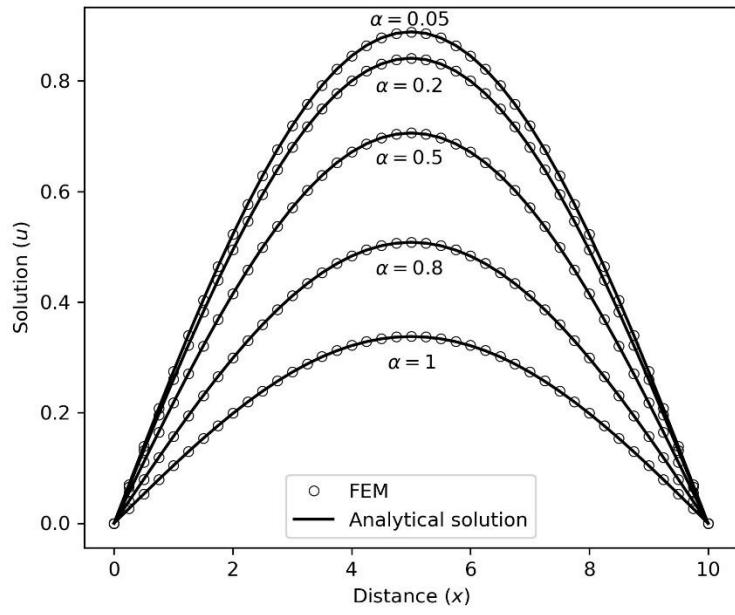
Figure 25
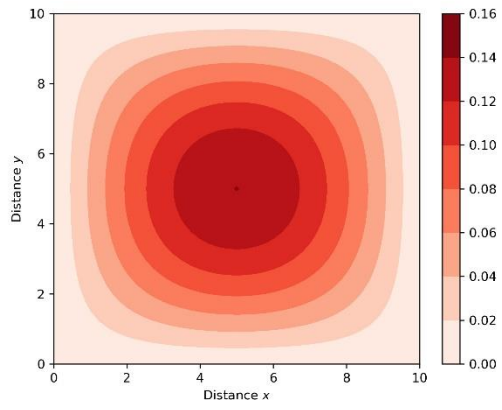
(a)
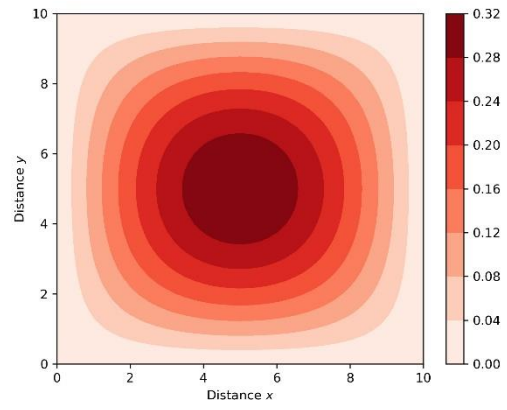
(b)

(c)
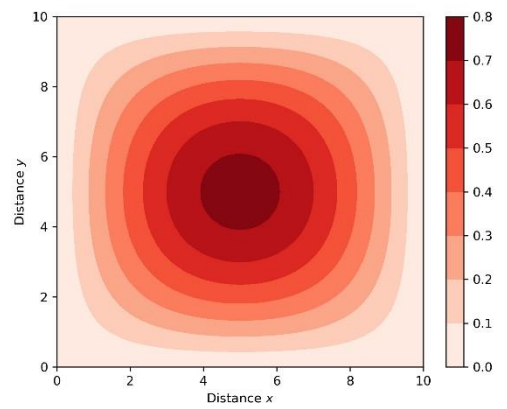
(d)

(e)

FIGURE 26

(a)

(b)

(c)

(d)

(e)

FIGURE 27